Materials Physics and Mechanics 27 (2016) 98-107 Received: October 24, 2016

NUMERICAL APPROXIMATIONS OF GREEN'S FUNCTIONS FOR ELASTIC ANISOTROPIC MEDIA BY SPHERICAL HARMONICS, INTERACTION ENERGIES OF POINT DEFECTS

R.S. Telyatnik

Institute for Problems in Mechanical Engineering of Russian Academy of Sciences,

Bolshoy pr. 61, V.O., Saint-Petersburg, 199178, Russia.

e-mail: statphys@ya.ru

Abstract. Fundamental solutions of elastostatics for infinite anisotropic media are obtained by numerical integration, and also by the finite element method for bounded sphere. These solutions are presented in the form of mean-squared approximation by the series of spherical harmonics Y_{lm} up to the order $l = 10$ (look for Online Support Data) as exemplified by the materials of different elastic symmetry: isotropic (concrete), cubic (Si), hexagonal (AlN), orthorhombic ($MgSiO_3$ in perovskite phase), tetragonal with 6 or 7 independent elastic constants ($ZrSiO_4$ and $CaWO_4$ respectively), trigonal with 6 or 7 constants (Al_2O_3 and dolomite), monoclinic (gypsum), triclinic (Al_2SiO_5). Using obtained Green's functions for each crystal, the energy of elastic interaction of a pair of point defects has been plotted as a function of angles of their mutual orientation.

1. Introduction

A fundamental solution, or Green's function, $G_{ij}(\vec{r})$ for static elastic field of an infinite medium is the r_i-component of displacement caused by unit point force applied in the origin of coordinates and acting along r_j-direction. Knowing the Green's function, one can obtain via the convolution integral a solution for an arbitrary distribution of forces in the medium, usually associated with the presence of inclusions, cracks, defects of the crystal lattice. Therefore, the Green's functions of a static elastic field got the main advancement in the continuum theory of defects in solids [1, 2], e.g. for calculation of various inclusions [3], dislocations and nanostructures [3]. An exact solution for the Green's function can be derived by the method of Fredholm [5] only for isotropic and hexagonal (transversely isotropic) media, that was realized for the first time by, respectively, Thompson (Lord Kelvin) [6] and Lifshitz with Rosenzweig [7]. For cubic media, the limited approximate solutions have been proposed using the perturbation theory in the presence of a small anisotropy parameter [7]. For various anisotropic media, numerical schemes have been developed to compute the Green's function and its derivatives by Meissner [9] and Barnett [9], that is detailed in the monography [1]. The effective numerical calculation is based herewith on the approach of Lifshitz and Rosenzweig, who were the first to reduce the triple integral to a single one [7].

The Green's function of an elastic medium can be expanded in a series of spherical harmonics $Y_{lm}(\theta,\varphi)$ comprising the orthonormal basis [11], that was first proposed by Burgers [12], moreover only components with even l have nonzero contribution, as it was shown by Mura and Kinoshita [14]. The expansion coefficients can be calculated via term-by-term series integration by spherical angles θ and φ using the basis orthonormal property [15], but it is more

© 2016, Institute of Problems of Mechanical Engineering

convenient to approximate the coefficients by the least square method for just once calculated Green's function on a grid of (θ, φ) values. This paper (+ Online Support Data) presents tabular and graphic results for the components of the Green's tensor functions in different anisotropic media exemplified by all possible crystal systems to clearly understand which coefficients of the expansion are the same, opposite or zero for each type of crystal symmetry.

An advantage of the easily differentiable expansion in spherical harmonics is provided by the fact that namely the derivatives of the Green's function have the main physical significance. In this paper, using the second derivatives, the energy of elastic interaction of a pair of point defects is plotted as a function of angles of their mutual orientation. This energy allows to understand dynamics and equilibrium locations of defects, and, in general, it is useful for characterization of an anisotropic medium by a scalar quantity.

The Green's function can be also numerically calculated by the finite element method (FEM) [16], that is also relevant to bounded or dynamic media [17]. Green's function method and FEM can effectively augment each other to reduce FEM residuals associated with nodal forces [18]. Analytic solutions are known only for a small number of boundary conditions, e.g. for half-spaces of isotropic (Mindlin [19]) and hexagonal media (Lee [20]). In the presence of boundaries or multipole point forces [21], the elastic field loses its simple decline with distance as $1/r$, therefore the expansions by vector spherical harmonics, which include additional radial dependencies, are used in this case. To estimate the Green's function for infinite media one should take quite large FEM model or approximate it with substraction of response displacements to sustain certain boundary conditions. Since elastic field caused by given displacements on a sphere is known analytically for isotropic case [23], it can be used in similar form for approximations in anisotropic media.

2. Anisotropic media

Anisotropy of an elastic medium is expressed by Hooke's law relating stress σ_{ij} with strain ε_{kl} tensor components via the stiffness coefficients: $\sigma_{ij} = c_{ijkl}\,\varepsilon_{kl}$ (summation over repeated indices). Due to the symmetry of the tensor c_{ijkl} under permutations of i and j, k and l, as well as pairs ij and kl, it is convenient to express the law of elasticity in Voigt notation ($1,\ldots,6 \leftrightarrow xx,yy,zz,yz,xz,xy$) using the symmetrical stiffness matrix, which has in general (triclinic) case 21 independent components [25]:

$$\begin{pmatrix} \sigma_{xx} \\ \sigma_{yy} \\ \sigma_{zz} \\ \sigma_{yz} \\ \sigma_{xz} \\ \sigma_{xy} \end{pmatrix} = \begin{pmatrix} c_{11} & c_{12} & c_{13} & c_{14} & c_{15} & c_{16} \\ & c_{22} & c_{23} & c_{24} & c_{25} & c_{26} \\ & & c_{33} & c_{34} & c_{35} & c_{36} \\ & & & c_{44} & c_{45} & c_{46} \\ & & & & c_{55} & c_{56} \\ & & & & & c_{66} \end{pmatrix} \begin{pmatrix} \varepsilon_{xx} \\ \varepsilon_{yy} \\ \varepsilon_{zz} \\ 2\varepsilon_{yz} \\ 2\varepsilon_{xz} \\ 2\varepsilon_{xy} \end{pmatrix}. \tag{1}$$

In the presence of a symmetry the amount of independent coefficients reduces to 13 in monoclinic symmetry, 9 in orthorhombic (orthotropic), 7 or 6 (depending on crystal class) in trigonal and tetragonal symmetries, 5 in hexagonal (transversely-isotropic), 3 in cubic and 2 in isotropic media. In the Tab. 1, the stiffness coefficients are presented with accentuation of dependent and zero components for each symmetry exemplified by following materials: constructional concrete; architectural gypsum $CaSO_4{*}2H_2O$; refractory dolomite $CaMg(CO_3)_2$ and kyanite Al_2SiO_5; magnesium silicate MgSiO3 dominating in Earth's lower mantle, that is important in seismology; zircon $ZrSiO_4$ – a metamict mineral indicating radioactive elements; calcium tungstate (scheelite) $CaWO_4$ used as scintillator and important ore of tungsten; silicon

Si and nitride aluminum AlN semiconductors, as well as insulator sapphire Al_2O_3, which serve as substrates for opto- and microelectronics.

Table 1. Stiffness coefficients (GPa) for materials of various symmetries.

	Al_2SiO_5	**Gypsum**	**Dolomite**	**Al_2O_3**	**AlN**	**$CaWO_4$**	**$ZrSiO_4$**	**$MgSiO_3$**	**Si**	**Concrete**
	tricl	monocl	trig7	trig6	hex	tetra7	tetra6	ortho	cub	isotr
	[26]*	[26]	[28]	[29]	[30]	[31]	[32]	[33]**	[34]	***
c_{11}	363.3	78.6	204.1	497	410	145.9	424.4	579	165.7	32.6
c_{12}	102.3	41.0	68.5	163	140	62.6	69.2	258	63.9	7.2
c_{13}	76.3	26.9	45.8	116	100	39.2	150.2	243	c_{12}	c_{12}
c_{14}	10.1	0	20.6	22	0	0	0	0	0	0
c_{15}	23.6	-7.0	6.7	0	0	0	0	0	0	0
c_{16}	7.0	0	0	0	0	-19.2	0	0	0	0
c_{22}	363.4	62.7	c_{11}	c_{11}	c_{11}	c_{11}	c_{11}	654	c_{11}	c_{11}
c_{23}	107.8	24.2	c_{13}	c_{13}	c_{13}	c_{13}	c_{13}	265	c_{12}	c_{12}
c_{24}	-21.8	0	$-c_{14}$	$-c_{14}$	0	0	0	0	0	0
c_{25}	1.0	3.1	$-c_{15}$	0	0	0	0	0	0	0
c_{26}	2.7	0	0	0	0	$-c_{16}$	0	0	0	0
c_{33}	363.3	72.6	97.4	501	390	127.4	489.6	615	c_{11}	c_{11}
c_{34}	-27.0	0	0	0	0	0	0	0	0	0
c_{35}	-13.7	-17.4	0	0	0	0	0	0	0	0
c_{36}	-6.1	0	0	0	0	0	0	0	0	0
c_{44}	164.0	9.1	39.1	147	120	33.5	113.3	232	79.6	Δc
c_{45}	-15.7	0	0	0	0	0	0	0	0	0
c_{46}	-2.4	-1.6	$-c_{15}$	0	0	0	0	0	0	0
c_{55}	103.7	26.4	c_{44}	c_{44}	c_{44}	c_{44}	c_{44}	210	c_{44}	Δc
c_{56}	1.9	0	c_{14}	c_{14}	0	0	0	0	0	0
c_{66}	120.9	10.4	Δc	Δc	Δc	38.7	48.2	178	c_{44}	Δc

$\Delta c = (c_{11} - c_{12})/2$

* Ab initio calculation ("from first-principles", i.e. by computational quantum chemistry).
** Ab initio calculation for perovskite phase under pressure 38 GPa and temperature 2500 °K.
*** Derived from Young modulus E = 30 GPa and Poisson coefficient ν = 0.18 in ANSYS material database.

3. Numerical calculation

The Green's function is a solution of equation of elastic equilibrium under a point unit force load (written in the right side of the equation via Kronecker delta and Dirac delta-function):

$$-c_{ijkl}\frac{\partial^2 G_{km}(\vec{r})}{\partial r_l \partial r_j} = \delta_{im}\delta(\vec{r}) \ . \tag{2}$$

Upon the Fourier transform of the equation (2), the Fourier transform of Green's function is expressed by the matrix inverse to the Green-Christoffel matrix $M_{ik} = c_{ijkl}\, h_j h_l$, where $\vec{h}$ is a unit vector in reciprocal space. So, the solution of (2) in real space is formally written as three-dimensional integral of inverse Fourier transform, which can be reduced to the following single integral [1]:

$$G_{ik}(r,\theta,\varphi) = \frac{1}{4\pi^2 r}\int_0^{\pi}\left(M^{-1}\right)_{ik}(\theta,\varphi,\psi)d\psi \ , \ M_{ik} = c_{ijkl}h_j h_l \ , \tag{3}$$

where the components of $\vec{h}(\theta,\varphi,\psi)$ have the following expression:

$$h_1 = \sin\varphi\cos\psi + \cos\theta\cos\varphi\sin\psi \ ,$$
$$h_2 = -\cos\varphi\cos\psi + \cos\theta\sin\varphi\sin\psi \ , \tag{4}$$
$$h_3 = -\sin\theta\sin\psi \ .$$

In this paper, the components of inverse Green-Christoffel matrix for general anisotropic (triclinic) case have been obtained by symbolic calculations in MATLAB package and presented in the appendix of the Online Support Data in text programmable manner for ability to copy-paste in numerical calculations for materials of your interest.

4. Analytic solutions

Derived by Kelvin [6], tensorial Green's function for an infinite isotropic medium can be rewritten from engineer elastic moduli in terms of stiffness coefficients as follows, where $c_{12} = vE/(1+v)/(1–2v)$, $c_{11} = (1–v)E/(1+v)/(1–2v)$ [25] and there is the isotropic relation for shear modulus $G = c_{44} = (c_{11}\text{-}c_{12})/2$:

$$G_{ij}^0(\vec{r}) = \frac{1}{8\pi r}\frac{c_{12}+c_{44}}{c_{44}\left(c_{12}+2c_{44}\right)}\left[\frac{c_{12}+3c_{44}}{c_{12}+c_{44}}\delta_{ij} + n_i n_j\right] \ , \ n_i = \frac{r_i}{r} \ . \tag{5}$$

For a cubic medium, the coefficient c_{44} is independent, so approximate expressions can be found by a perturbation theory with small parameter of deviation of c_{44} from isotropic value. Lifshitz and Rosenzweig [7] were the first who derived such expansion in first order for a cubic medium, but they made a mistake missing some terms, that was noticed by Dederichs and Leibfried [8] who derived a bit another expansion from isotropic averages of elastic constants. Following the logic of Lifshitz and Rosenzweig, Ostapchuk corrected their mistake [35] and derived the following expansion, using the designations in (5):

$$G_{ij}^{\text{cub}}(\vec{r}) \approx G_{ij}^0(\vec{r}) + \eta G_{ij}^1(\vec{r}) \ , \ \ \eta = \frac{c_{11}-c_{12}}{c_{44}} - 2 \ << \ 1, \tag{6}$$

$$G_{ij}^1(\vec{r}) = -\frac{1}{64\pi r}\frac{c_{12}+c_{44}}{c_{44}\left(c_{12}+2c_{44}\right)}\left[4c_{44}\frac{c_{12}+3c_{44}}{c_{12}+c_{44}}\left(1-n_i^2\right)\delta_{ij} + \left(7c_{12}+19c_{44}\right)n_i n_j - \right.$$
$$\left. -2\left(c_{12}+4c_{44}\right)n_i n_j\left(n_i^2+n_j^2\right) + \left(c_{12}+c_{44}\right)\left(1+\sum_{k=1}^{3}n_k^4\right)\delta_{ij} - 5\left(c_{12}+c_{44}\right)n_i n_j\sum_{k=1}^{3}n_k^4\right].$$

For a hexagonal medium, Lifshitz and Rosenzweig in the same paper [7] first derived correct exact solution. Let's rewrite it with explicit spherical coordinates using the following designation of square elastic constants

$$b_{1,2} = b_6 \pm b_3 \ , \ \ b_3 = \sqrt{b_6^2 + 4b_5 b_4} \ , \ b_4 = c_{11}c_{44} \ , \ b_5 = b_6 + c_{11}c_{44} - c_{33}c_{44} \ ,$$
$$b_6 = c_{11}c_{33} - 2c_{11}c_{44} - c_{13}^2 - 2c_{13}c_{44} \ , \tag{7}$$

and functions of spherical angle θ

$$q(\theta) = 2\left(b_4 + b_6\sin^2(\theta) - b_5\sin^4(\theta)\right) \ ,$$
$$p_i(\theta) = 2b_4 + b_i\sin^2(\theta) \ , \tag{8}$$
$$A(\theta) = \cos^2(\theta) + c_{44}/c_{66}\cdot\sin^2(\theta) \ ,$$
$$B_i(\theta) = \frac{1}{c_{66}}\left(\frac{c_{44}\left(c_{11}+c_{12}\right)}{2}\frac{1}{\sqrt{p_i(\theta)}} + \frac{b_6 + (2-c_{44}/c_{66})b_4 - c_{66}c_{33}}{A(\theta)\,p_i(\theta) - q(\theta)}\sqrt{p_i(\theta)}\sin^2(\theta)\right) \ , \tag{9}$$

then, the components of tensorial Green's function can be written as follows:

$$G_{\alpha j}^{\mathrm{hex}}(\vec{r})\cdot 4\pi r\sin^2(\theta)=-\left\{\frac{\cos^2(\theta)}{c_{44}\sqrt{A(\theta)}}+\frac{\sqrt{q(\theta)}}{b_3}\sum_{i=1}^{2}(-1)^i B_i(\theta)\right\}\delta_{\alpha j}+\left\{\frac{A(\theta)+\cos^2(\theta)}{c_{44}\sqrt{A(\theta)}}+\right. \tag{10}$$

$$\left.+\frac{1}{b_3\sqrt{q(\theta)}}\sum_{i=1}^{2}(-1)^i B_i(\theta)\left(q(\theta)+p_i(\theta)\cos^2(\theta)\right)\right\}\left(\cos(\varphi)\delta_{1\alpha}+\sin(\varphi)\delta_{2\alpha}\right)\left(\cos(\varphi)\delta_{1j}+\sin(\varphi)\delta_{2j}\right)-$$

$$-\frac{c_{13}+c_{44}}{b_3\sqrt{q(\theta)}}\cos(\theta)\sin(\theta)\left(\cos(\varphi)\delta_{1\alpha}+\sin(\varphi)\delta_{2\alpha}\right)\delta_{3j}\sum_{i=1}^{2}(-1)^i\sqrt{p_i(\theta)}\ ,\quad \alpha=1,2,$$

$$G_{3j}^{\mathrm{hex}}(\vec{r})\cdot 4\pi r\sin^2(\theta)=-\frac{1}{b_3\sqrt{q(\theta)}}\left\{\left(c_{13}+c_{44}\right)\cos(\theta)\sin(\theta)\left(\cos(\varphi)\delta_{1j}+\sin(\varphi)\delta_{2j}\right)\times\right. \tag{11}$$

$$\left.\times\sum_{i=1}^{2}(-1)^i\sqrt{p_i(\theta)}+\left[\left(c_{44}\sin^2(\theta)+c_{11}\cos^2(\theta)\right)\sum_{i=1}^{2}(-1)^i\sqrt{p_i(\theta)}-c_{11}q(\theta)\sum_{i=1}^{2}\frac{(-1)^i}{\sqrt{p_i(\theta)}}\right]\delta_{3j}\right\}.$$

This solution is applicable for such relation of the elastic constants that gives positive sign in subradicals. The opposite case was considered by analogy by Lejček [36]. Another treatments and appearances of the Green's function for a hexagonal medium were also obtained by Kröner [13] (with mistake in a factor), Willis [36], Pan and Chou [38] (with wrong expressions for components corresponding to the force parallel to the XY-plane of isotropy).

5. Approximations by spherical harmonics

The Green's function of an infinite elastic medium is factorized into the radial part descending as $1/r$ and the angular part which can be expanded in the series [2]

$$G_{ij}(r,\theta,\varphi)=\frac{1}{r}\sum_{l=0,2,4,\ldots}^{\infty}\sum_{m=-l}^{l}a_{lm}^{(ij)}Y_{lm}(\theta,\varphi) \tag{12}$$

by the orthonormal basis of spherical harmonics [11]

$$Y_{lm}(\theta,\varphi)=\sqrt{\frac{2l+1}{2\pi}\frac{(l-|m|)!}{(l+|m|)!}}P_{lm}(\cos(\theta))\cdot\begin{cases}\cos(m\varphi),\ m>0\\ \sin(-m\varphi),\ m<0,\\ 1/\sqrt{2},\ m=0\end{cases} \tag{13}$$

where the associated Legendre polynomials are defined:

$$P_{lm}(x)=\frac{(-1)^m}{2^l l!}\left(1-x^2\right)^{m/2}\frac{d^{l+m}}{dx^{l+m}}\left(x^2-1\right)^l,\ 0\le m\ ,$$
$$P_{l,-m}(x)=(-1)^m\frac{(l-m)!}{(l+m)!}P_{l,m}(x),\ 0\le m\le l\ . \tag{14}$$

In this paper, for each component of G_{ij}, the approximation up to the order $l = 12$ with 91 coefficients a_{lm} has been carried out by MATLAB function *fit* for the integral values (3) calculated by the function *integral* with a precision not worse than 10^{-17} m^2/N for a coordinate grid (θ, φ) with 1° resolution (Fig. 1). This resolution provides approximation of a_{lm} with the exceeding accuracy ~10^{-19} m^2/N (the width of 95 % confidence interval) to account about one hundred terms in the expansion. The results for all materials from tab. 1 are presented with round-off in the tables 2-11 in the Online Support Data up to the order $l = 10$, therewith all omitted components are zero, namely all $a_{lm} = 0$ with $l < 0$ for $G_{11,\,22,\,33,\,13}$ and with $l \ge 0$ for $G_{12,\,23}$ for every symmetry except triclinic, trigonal, and tetragonal with 7 constants. Illustrative graphics of Green's tensor components are presented below for isotropic concrete (Figs. 1, 2) and trigonal dolomite (Figs. 1, 3).

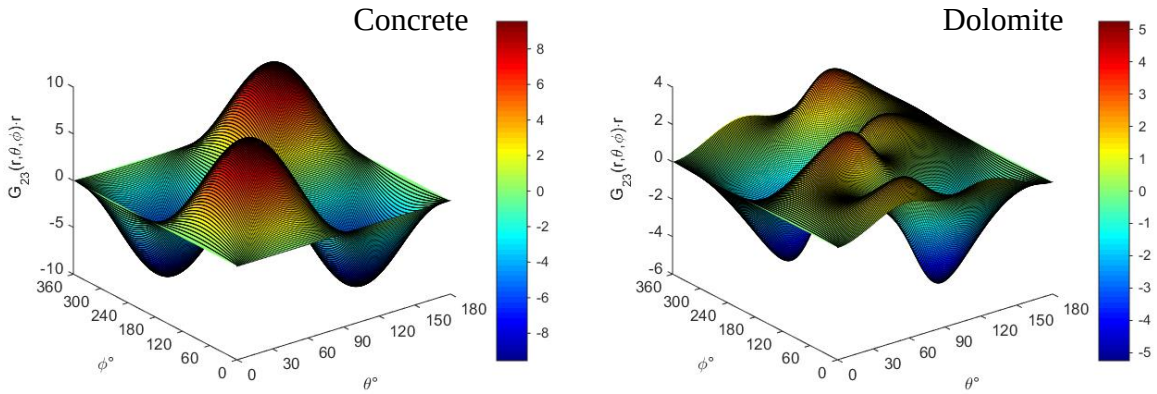

Fig. 1. Examples of approximated surface $G_{23}(r,\theta,\varphi)\cdot r$ (colored height, 10^{-13} m^2/N) for the 1°-resolution mesh of numerical solutions.

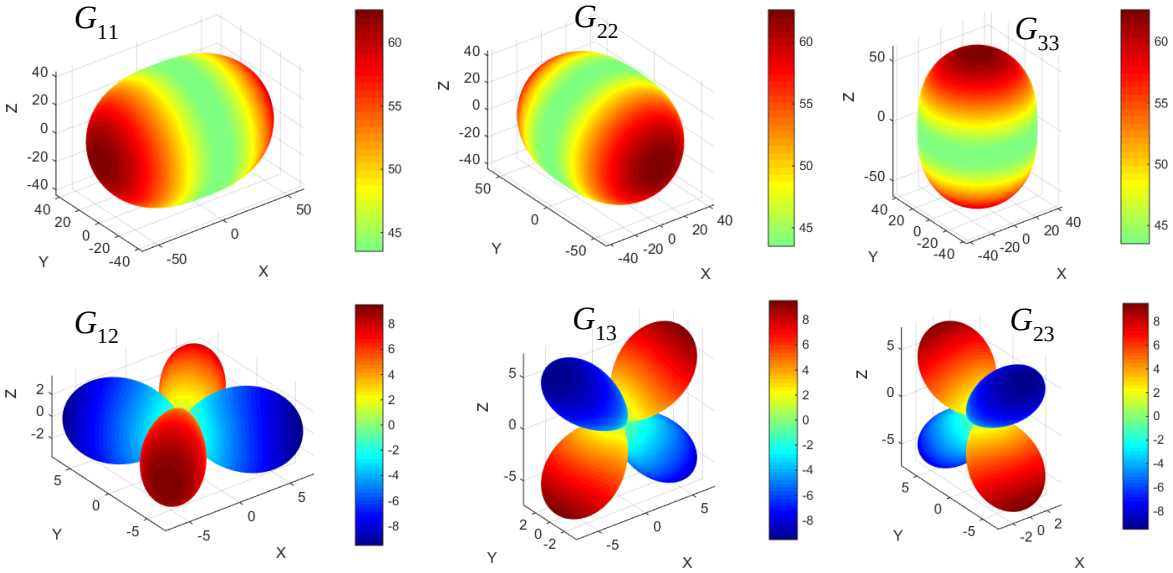

Fig. 2. Surfaces (X,Y,Z) = $G_{ij}(\vec{r})\cdot\vec{r}$ (10^{-13} m^2/N) for isotropic concrete. The color designates the value of radius-vector with account of G_{ij} sign.

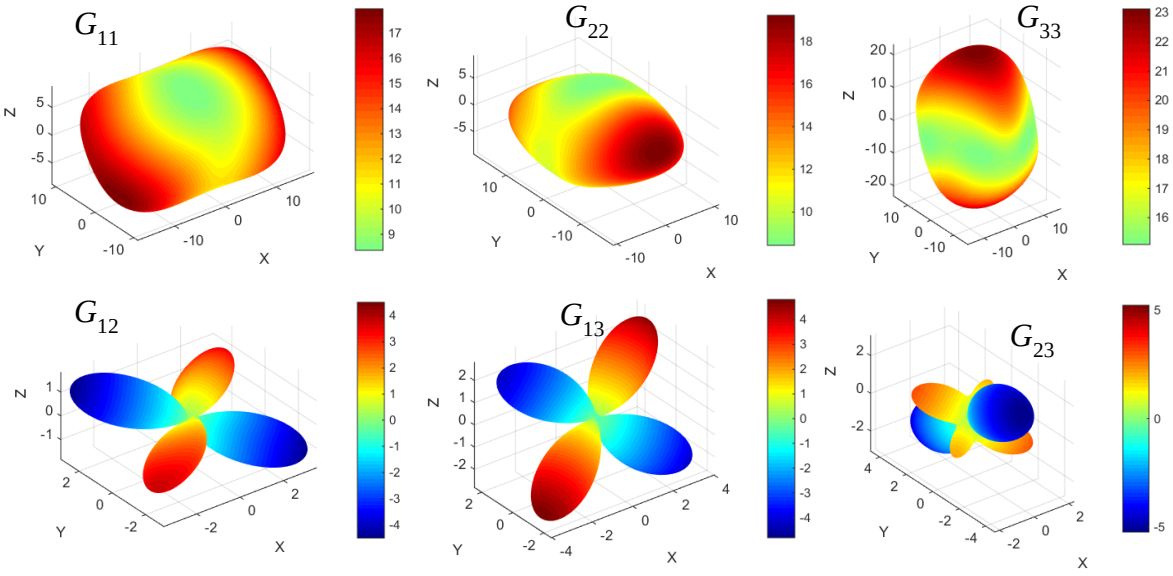

Fig. 3. Surfaces (X,Y,Z) = $G_{ij}(\vec{r})\cdot\vec{r}$ (10^{-13} m^2/N) for trigonal dolomite.

6. Finite-element solution

Since FEM model is finite, it is convenient to model it as a sphere of radius R with zero displacements on its boundary. For isotropic medium (with Poisson coefficient ν), if a displacement $\vec{U}(\vec{r})$ is imposed on the spherical surface, than the analytic solution for corresponding displacement field has following expansion in spherical harmonics:

$$u_i^{\mathrm{R}}(\vec{r}) = \sum_{l=0}^{\infty}\left[\delta_{ik} + \frac{R^2 - r^2}{2\left(3l - 2 - 2\nu\left(2l-1\right)\right)}\frac{\partial}{\partial r_i}\sum_{k=1}^{3}\frac{\partial}{\partial r_k}\right]\left(\frac{r}{R}\right)^l U_k^{(l)}(\vec{r}) \ , \quad r < R$$
$$U_i^{(l)}(\vec{r}) = \sum_{m=-l}^{l}\tilde{a}_{lm}^{(i)} Y_{lm}(\theta,\varphi) \ , \quad r = R \tag{15}$$

One can find derivation of this result in Lurie monographs from general solution representations in Papkovich-Neuber [23] or Trefftz form [24]. For anisotropic media, (15) may be approximated with some effective coefficient ν or, in general, with factors to each given coefficient $\tilde{a}_{lm}^{(i)}$. Due to superposition of small strains, the Green's function G_{ij} for infinite medium can be extracted from the FEM solution on the Green's function G_{ij}^{R} for the force acting in the center of the finite sphere (in j-direction). To obey zero displacements on the boundary, the components of external displacement $U_{i(j)}$ with expansion coefficients $\tilde{a}_{lm}^{(ij)}$ must be precisely opposite to G_{ij} with coefficients $a_{lm}^{(ij)}$:

$$G_{ij}^{\mathrm{R}}(\vec{r}) = G_{ij}(\vec{r}) + u_{i(j)}^{\mathrm{R}}(\vec{r}\,|\vec{U}_{(j)}) \ , \quad U_{i(j)}(\vec{r}) = -G_{ij}(r = R, \theta, \varphi) \tag{16}$$

Thus, the mean-squared approximation of a non-linear regression (MATLAB function *nlinfit*) can be used to determine $a_{lm}^{(ij)}$ and ν by fitting the surface of FEM nodal solutions G_{ij}^{R} in 4-dimensional space (G, x, y, z) by model function (16). However, this is not very efficient procedure since it requires simultaneous approximation of G_{1j}, G_{2j}, G_{3j} according to the gradient in (15) and it requires representative selection of numerous nodal solutions of FEM mesh to approximate angular and radial dependencies without rank deficient problems. So it is more useful to make independent G_{ij} approximations for angular dependencies by taking a quite large sphere, e.g. R = 1000 m, with dense FEM mesh up to r~1 m and approximate only spherical components around the unit sphere knowing that $(r/R)^l$ in (15) produces ~0.1 % error for scalar component a_{00} and much less for angular ones with l = 2,4,… At that, instead of nearby nodal displacements, it is recommended to use interpolational values strictly on the unit sphere. ANSYS software with Mechanical APDL module provides the tool to evaluate interpolation on (θ, φ)-grid on a sphere with necessary resolution. While utilising ANSYS, we recommend to use direct mesh operations instead of *multibody part* sections to define central node to apply a force. Try *Mesh*-options *Use Advanced Size Function* with *Sizing Type – Sphere of Influence* to build automatic mesh of higher-order tetrahedral elements SOLID187 condensing towards the center.

Figure 4 shows how G_{ii}^{R} deviates from G_{ii} while reaching spherical boundary with zero displacement by the example of hexagonal AlN. FEM solution coincides with the approximation (16) by spherical harmonics for G_{ii} and coefficient ν = 0.252 for G_{11}^{R}, G_{22}^{R} and ν = 0.238 for G_{33}^{R} (for comparison, orthotropic Poisson coefficients for AlN are ν_{xy} = 0.298 and $\nu_{xz} = \nu_{yz}$ = 0.180). For G_{ij} with $i \neq j$, which have a_{00} = 0 in expansions by spherical harmonics in all crystal symmetries except triclinic and monoclinic, there is no special need to correct the next order l = 2 with any certain value of parameter ν slightly affecting only close boundary vicinity. Though one should be careful with small angular errors of Green's function, which can lead to great deviations of the function derivatives, that is essential for such problems as following.

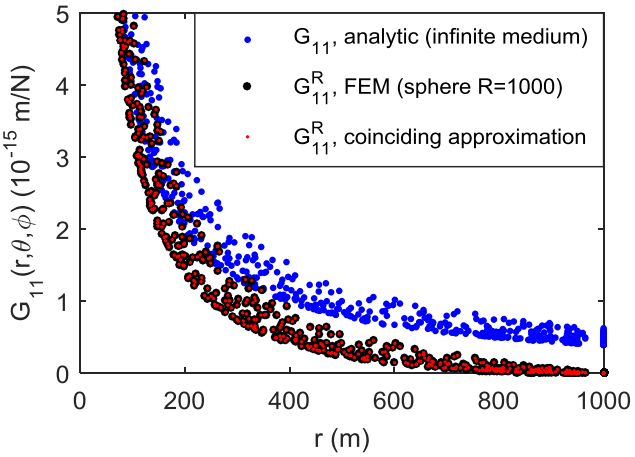

Fig. 4. G_{11} and G_{11}^{R} radial dependencies at random angles for hexagonal AlN.

7. Point defects interaction energy

Let a point defect to produce in anisotropic medium a spherically symmetric field of forces, which can be determined as follows, where K is bulk modulus (expressed by stiffness coefficients [25]), and ΔV is volume change of the medium caused by the defect formation [39]:

$$f_i(\vec{r}) = K\Delta V \frac{\partial}{\partial r_i}\delta(\vec{r}) \tag{17}$$

The displacements are evaluated via spatial convolution of the forces with the Green's function (summation over repeated indices):

$$u_j(\vec{r}) = \int G_{ij}(\vec{r}-\vec{r}')\, f_i(\vec{r}')d\vec{r}' = -K\Delta V \frac{\partial G_{ij}(\vec{r})}{\partial r_i}. \tag{18}$$

The first derivatives of displacements determine the strains, which in turn determine the stresses via the Hook's law. Then, the energy can be expressed for the defect in the stress field of another similar defect [39]:

$$E_{\text{int}}(\vec{r}) = -K\Delta V^{\text{II}}\varepsilon_{jj}^{\text{I}}(\vec{r}) = K^2\Delta V^{\text{I}}\Delta V^{\text{II}}\frac{\partial^2 G_{ij}(\vec{r})}{\partial r_i \partial r_j} = K^2\Delta V^{\text{I}}\Delta V^{\text{II}}\frac{1}{r^3}U(\theta,\varphi) \tag{19}$$

It is known from analytic solutions that E_{int} is zero for an infinite isotropic medium, while this energy doesn't depend on φ in transversely-isotropic (hexagonal) medium [40]. In anisotropic media, there are always coexisting (θ, φ) directions, in which E_{int} is positive (the defects repel each other) and negative (the defects attract each other). The interaction energies of the point defects in each material from Tab. 1 are calculated using the approximated numerical solutions of the Green's functions and presented by the outline maps of $U(\theta,\varphi)$ from (19) (Fig. 5), by which one can easily see the symmetry imposed by the medium on the interaction energy:

All media, including triclinic: $U(\theta,\varphi) = U(\theta+\pi,\varphi)$, $U(\theta,\varphi) = U(-\theta,\varphi+\pi)$.
Monoclinic: $U(\theta,\varphi) = U(\theta,-\varphi)$.
Trigonal: $U(\theta,\varphi) = U(-\theta,\varphi+\pi/3)$.
Orthotropic: $U(\theta,\varphi) = U(-\theta,\varphi)$, $U(\theta,\varphi) = U(\theta,\varphi+\pi)$.
Tetragonal and cubic: $U(\theta,\varphi) = U(-\theta,\varphi)$, $U(\theta,\varphi) = U(\theta,\varphi+\pi/2)$.

On the poles $\theta = 0, \pi$, all crystal systems except triclinic and monoclinic have extremum of $U(\theta,\varphi)$, usually global.

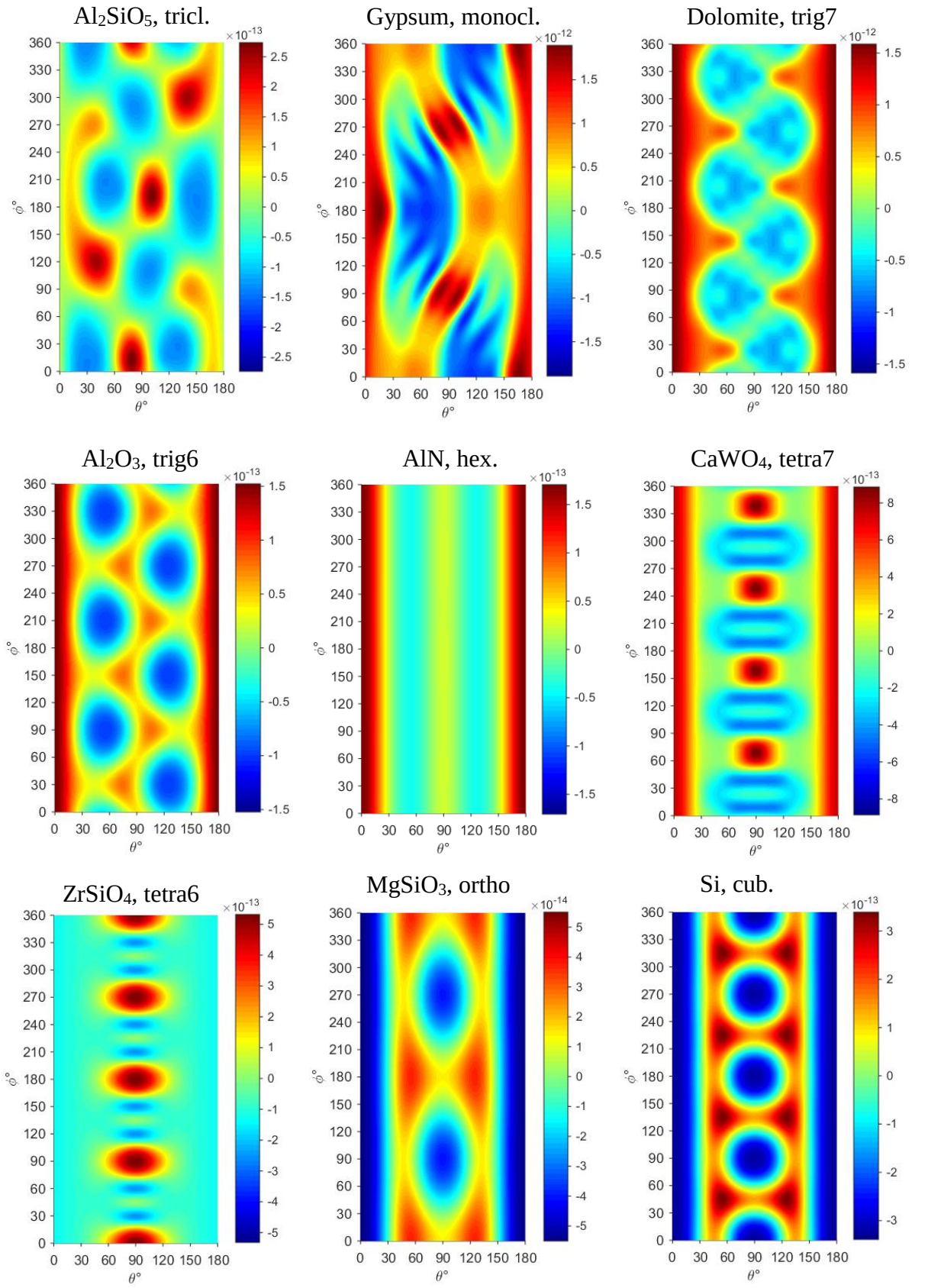

Fig. 5. $U(\theta,\varphi)$ (by color, m^2/N), the patterns of interaction energy of two point defects in various anisotropic media (Tab. 1).

Acknowledgements. *This work is supported by the grant of Russian president MK-5261.2014.1 and by the RFBR grants № 15-03-06155, № 16-29-03149 ofi_m.*

References

[1] C. Teodosiu, *Elastic Models of Crystal Defects* (Springer-Verlag, Berlin Heidelberg, 1982).
[2] T.Mura, *Micromechanics of Defects in Solids* (Martinus Nijhof Publishers, Dordrecht,1987).
[3] I.A. Ovid'ko, A.G. Sheinerman // *Materials Physics and Mechanics* **10** (2010) 1.
[4] M.Yu. Gutkin, I.A. Ovid'ko, A.G. Sheinerman // *Journal of Physics: Condensed Matter* **15** (2003) 3539.
[5] I. Fredholm // *Acta Mathematica* **23** (1900) 1.
[6] W. Thompson // *The Cambridge and Dublin Mathematical Journal* **3** (1848) 87.
[7] I.M. Lifshitz, L.N. Rosenzveig // *ZhETF* **17** (1947) 9. (In Russian).
[8] P.H. Dederichs, G. Leibfried // *Physical Review* **188** (1969) 1175.
[9] N. Meissner // *AERE Report, TP* (1973) 556.
[10] D.M. Barnett // *Physica Status Solidi B* **49** (1972) 741.
[11] E.W. Hobson, *The Theory of Spherical and Ellipsoidal Harmonics* (Cambridge University Press, 1931).
[12] J.M. Burgers // *Proceedings of the Koninklijke Nederlandse Akademie van Wetenschappen* **42** (1939) 378.
[13] E. Kröner // *Zeitschrift fur Phyzik* **136** (1953) 402.
[14] T. Mura, N. Kinoshita // *Physica Status Solidi B* **47** (1971) 607.
[15] R.K. Leutz, R. Bauer // *Computer Physics Communications* **11** (1976) 339.
[16] T.J.R. Hughes, *The Finite Element Method: Linear Static and Dynamic Finite Element Analysis* (Prentice-Hall, 1987).
[17] D. Duhamel // *Engineering Analysis with Boundary Elements* **31** (2007) 919.
[18] F.G. Hartmann, *Green's Functions and Finite Elements* (Springer-Verlag, Berlin Heidelberg, 2013).
[19] R.D. Mindlin // *Physics* **7** (1936) 195.
[20] N.G. Lee // *International Journal of Engineering Science* **17** (1979) 681.
[21] R.-P. Hirsekorn, R. Siems // *Z. Phys. B.* **47** (1982) 155.
[22] Y.Y. Kagan // *Geophys. J. R. astr. SOC.* **90** (1987) 1.
[23] A.I. Lur'e, *Three-Dimensional Problems of the Theory of Elasticity* (Interscience, New York, 1964).
[24] A.I. Lur'e, *Theory of Elasticity* (Nauka, Moscow, 1970). (In Russian).
[25] J.F. Nye, *Physical Properties of Crystals* (Clarendon Press, Oxford, 1957).
[26] H. Yao, L. Ouyang, W.-Y.Ching // *Journal of the American Ceramic Society* **90** (2007) 3194.
[27] S. Haussuhl // *Zeitschrift für Kristallographie* **122** (1965) 311.
[28] P.-F. Chen, L.-Y. Chiao, P.-h. Huang, Y.-j. Yang, L.-g. Liu // *Physics of the Earth and Planetary Interiors* **155** (2006) 73.
[29] D.B. Hovis, A. Reddy, A.H. Heuer // *Applied Physics Letters* **88** (2006) 131910
[30] C. Deger, E. Born, H. Angerer, O. Ambacher, M. Stutzmann // *Applied Physics Letters* **72** (1998) 2400.
[31] J.M. Farley, G.A. Saunders // *Journal of Physics C: Solid State Physics* **5** (1972) 3021.
[32] H. Özkan, L. Cartz, J.C. Jamieson // *Journal of Applied Physics* **45** (1974) 556
[33] A.R. Oganov, J.P. Brodholt, G.D. Price // *Nature* **411** (2001) 934.
[34] H.J. McSkimin // *Journal of Applied Physics* **24** (1953) 988.
[35] P.N. Ostapchuk // *Physics of the Solid State* **54(1)** (2012) 98.
[36] L. Lejček // *Czechoslovak Journal of Physics B* **19** (1969) 799.
[37] J.R. Willis // *The Quarterly Journal of Mechanics and Applied Mathematics* **18** (1965) 419.
[38] Y.-C. Pan, T.-W. Chou // *Journal of Applied Mechanics* **46** (1979) 551.
[39] A.M. Kosevich, *Fundamentals of the Crystal Lattice Mechanics* (Nauka, Moscow, 1972). (In Russian).
[40] S.A. Kukushkin, A.V. Osipov, R.S. Telyatnik // *Physics of the Solid State* **58(5)** (2016) 941.